

Article

Adsorption Removal of Phosphate from Rural Domestic Sewage by Ca-Modified Biochar Derived from Waste Eggshell and Sawdust

Cancan Xu ^{1,2}, Rui Liu ^{2,*}, Qi Tang ³, Yifan Hou ¹, Lvjun Chen ^{2,4} and Quanxi Wang ^{5,*}

¹ School of Environmental and Geographical Sciences, Shanghai Normal University, Shanghai 200234, China; xucancan523127@126.com (C.X.); yifann0918@163.com (Y.H.)

² Zhejiang Provincial Key Laboratory of Water Science and Technology, Department of Environment in Yangtze Delta Region Institute of Tsinghua University, Jiaxing 314006, China; chenlj@tsinghua.edu.cn

³ School of Environment and Engineering, Changzhou University, Changzhou 213614, China; tangqi9866@126.com

⁴ School of Environment, Tsinghua University, Beijing 100084, China

⁵ College of Life Science, Shanghai Normal University, Shanghai 200234, China

* Correspondence: liuruitsinghuazj@gmail.com (R.L.); wangqx@shnu.edu.cn (Q.W.); Tel.: +86-0573-82581603 (R.L.)

Abstract: In recent years, in order to improve the rural living environment, rural domestic sewage treatment has received more and more attention in China. However, the standard compliance rate of total phosphorus (TP) in rural domestic sewage after treatment is very low, and TP has become the main pollutant that prevents rural domestic sewage treatment facilities from meeting water pollutants discharge standards. In this study, to prepare calcium-modified biochar composites (E-BC) by one-step pyrolysis, waste eggshell (E) was employed as a calcium source and waste pine sawdust (BC) was employed as a carbon source. The E-BC composites produced were effective in adsorbing phosphate (P) from aqueous solutions in a broad pH range of 3–11, with good adsorption selectivity. E-BC's adsorption capacity for P increased as the pyrolysis temperature increased from 700 °C to 900 °C, which was attributed to the higher specific surface area and calcium oxide content at higher pyrolysis temperatures. The E-BC sample, which was made from eggshell (filtered through 100 mesh sieves) and pine sawdust (filtered through 100 mesh sieves) with a mass ratio of 2:1 and a pyrolysis temperature of 900 °C, had a maximum adsorption capacity of 301 mg/g. The Langmuir model and pseudo second-order model were the best at describing the adsorption process, and the predominant sorption mechanism for P is the chemisorption reaction of calcium oxide or calcium hydroxide with phosphate to create hydroxyapatite. E-BC can effectively remove P from rural domestic sewage. The total phosphorus (TP) removal rate in rural domestic sewage ranges from 95.3 to 99.5%. After adsorption treatment, the discharge of TP in rural sewage meets the second-grade (TP < 3 mg/L) or even the first-grade (TP < 2 mg/L). This study provides an experimental basis for efficient P removal using E-BC adsorbent materials and suggests possible applications in rural domestic sewage.



Citation: Xu, C.; Liu, R.; Tang, Q.; Hou, Y.; Chen, L.; Wang, Q. Adsorption Removal of Phosphate from Rural Domestic Sewage by Ca-Modified Biochar Derived from Waste Eggshell and Sawdust. *Water* **2023**, *15*, 3087. <https://doi.org/10.3390/w15173087>

Academic Editor: Laura Bulgariu

Received: 20 July 2023

Revised: 23 August 2023

Accepted: 24 August 2023

Published: 28 August 2023



Copyright: © 2023 by the authors. Licensee MDPI, Basel, Switzerland. This article is an open access article distributed under the terms and conditions of the Creative Commons Attribution (CC BY) license (<https://creativecommons.org/licenses/by/4.0/>).

1. Introduction

In recent years, in order to improve the rural living environment, rural domestic sewage treatment has received more and more attention by the Chinese government. The most conventional treatment methods for domestic sewage in rural regions consist of an operational sequence of aerobic/anoxic/aerobic processes. Anaerobic-Anoxic-Oxic (A²O) is one of the most typical schemes in China. However, some reports have observed that the efficient removal of COD, NH₃-N, and total phosphorus (TP) is hard to realize [1]. In the study by Yang et. al., centralized rural sewage treatment facilities surrounding Erhai Lake in Yunnan Province had good removal efficiency. However, certain centralized sewage

treatment facilities have been unable to meet the required standards for water pollution discharge, with a particularly low average compliance rate of only 4.26% for TP. Therefore, determining how to improve TP treatment efficiency to meet discharge standards in rural regions is an important target of future research [2].

Different biological, chemical, and physical techniques have been created and widely applied in previous studies to manage and treat the phosphorus present in wastewater [3–5]. Out of all the methods available, the adsorption technique is the most appealing due to its economic feasibility and ease of application in the real world. In addition, the nutrient-loaded adsorbents can be further utilized as soil conditioners and fertilizers [6]. Biochar is recognized as an eco-friendly and potentially low-cost adsorbent material as it has excellent physicochemical properties and is considered to be a potential soil amendment [7]. Pure biochar is effective at adsorbing organic pollutants and cations; however, its ability to adsorb phosphorus is limited [8]. The presence of a high proportion of phenolic and carboxylic groups in the biochar makes the biochar's surface negatively charged, preventing the adsorption of phosphates [9,10]. To improve the adsorption property of phosphates, the biochar must be modified. Calcium (Ca), which is an environmentally friendly, cheap, and widely abundant metal, could effectively remove phosphate (P) from solution [11–13]. Ca loaded on other carrier materials, such as biochar, can be effective adsorbents for the recovery of phosphorus from wastewater [14]. The traditional Ca-modified biochar methods utilize the chemical reagents calcium hydroxide (Ca(OH)_2), calcium carbonate (CaCO_3), or calcium chloride (CaCl_2) as Ca sources [15,16]. The cost of raw materials for adsorbents is one of the important factors influencing their practical application. Recently, the development of adsorbents using waste biomass as preparation raw materials has received extensive attention [17].

Eggshells contain CaCO_3 (~94%) and organic matter (~6%) [18]. Globally, 8.6 million metric tons of eggshell waste had been produced by 2018 [19]. Despite the fact that eggshells are typically thrown away as kitchen waste, they are a valuable feedstock that may be used in a variety of other ways [20,21]. For example, the carbon dioxide (CO_2) from the decomposition of CaCO_3 in eggshells can be used to activate substances and produce activated carbon [22]. Additionally, eggshells have the potential to be a source of calcium for the creation of Ca-modified biochar since they have the ability to absorb phosphorus and then be used as a phosphate fertilizer [23,24]. Sawdust is a by-product generated from wood processing. Industries such as carpentry, furniture making, dimension mills, cabinet making, and sawmills are major producers of sawdust [25]. In fact, sawdust makes up more than 40% of the lignocellulosic residues produced by industrial forest processing, which totals 180 million m^3 globally [26]. However, sawdust is often used in low-value-added applications or acts as forest waste [27]. From environmental and bioeconomic points of view, it is important to convert low-value sawdust into value-added products through a sustainable processing approach. The carbonized sawdust forms a material with abundant surface functional groups and stable structure; these characteristics demonstrate that sawdust is a good substrate to produce biochar. The removal of P in wastewater from cattle farm, pond, pig farm, and human urine by Ca-modified biochar has been reported [14,17]. So far, the reports on the P treatment of rural domestic sewage by calcium-modified biochar are limited. In addition, the mass ratio, size, and pyrolysis temperature of the raw material (waste biomass) are important factors affecting the P adsorption performance of Ca-modified biochar. However, so far, there are few reports on the comprehensive optimization of the ratio, size, and pyrolysis temperature of raw matter (waste biomass) to improve the P removal performance of Ca-modified biochar.

In this study, in order to improve TP treatment efficiency for meeting discharge standards in rural regions and optimize the synthetic conditions of Ca-modified biochar from natural waste, waste eggshell was used as the Ca source, and sawdust waste as the carbon (C) source to synthesize biochar composite (E-BC) through one-step pyrolysis. The mass ratio of eggshell and sawdust, the powder size of eggshell and sawdust, and the pyrolysis

temperature were optimized to improve the P sorption capacity in aqueous solution of E-BC. Some adsorption models were used to observe the adsorption performance of P by E-BC. The mechanisms of P adsorption on the prepared E-BC were analyzed. The feasibility of E-BC as an adsorbent for TP removal was also assessed using rural domestic sewage. This study suggests possible applications in rural domestic sewage.

2. Materials and Methods

2.1. Experimental Materials

Pine sawdust was obtained from a timber factory in Jiaxing (China). Before use, it was dried at 60 °C in an oven, ground with a grinding machine, and passed through 20–100 mesh sieves (0.85–0.15 mm). Waste eggshells were obtained from a mess hall of Jiaxing and were dried at 60 °C in an oven after cleaning three times. They were then ground and passed through 20–100 mesh sieves (0.85–0.15 mm) before use. All chemical reagents (such as KH₂PO₄, HCl, NaOH, KCl, KNO₃, K₂SO₄, and KHCO₃) were analytical grade and purchased from Aladdin Industrial Corporation.

2.2. Preparation of Adsorbents

The mixture of eggshell (through 40 mesh sieves) and pine sawdust (through 40 mesh sieves) powder at a weight ratio of 3:1, 2:1, 1:1, and 1:2 was transferred to a quartz boat, and then the mixture of eggshell and pine sawdust was calcined in the tube furnace for 2 h under a nitrogen atmosphere at 800 °C. The mixture of eggshell (through 20–100 mesh sieves) and pine sawdust (through 20–100 mesh sieves) powder at a weight ratio of 2:1 was transferred to a quartz boat, and then calcined for 2 h in the tube furnace under a nitrogen atmosphere at 800 °C. The mixture of eggshell (through 100 mesh sieves) and pine sawdust (through 100 mesh sieves) powder at a weight ratio of 2:1 was transferred to a quartz boat, and then calcined for 2 h in the tube furnace under a quartz atmosphere at 700 °C and 900 °C. The heating rate was 5 °C/min.

According to the weight ratio of eggshell (E) and pine sawdust (BC), the samples were named E-BC (3:1), E-BC (2:1), E-BC (1:1), and E-BC (1:2). According to the calcination temperature, the samples (eggshell powder passed through 100 mesh sieves and pine sawdust powder passed through 100 mesh sieves) were named E-BC (2:1)-T700, E-BC (2:1)-T800, and E-BC (2:1)-T900, respectively. Pure pine sawdust-prepared biochar was named BC.

2.3. Phosphate Adsorption Experiments

In this study, all adsorption experiments were carried out in batches. Typically, E-BC material was placed in a 100 mL glass vial containing 50 mL of phosphorus solutions with a stopper. The vials were oscillated (180 rpm) in a shaker bath (HZQ-F100 Jiangsu) at pH 7 and 25 °C. The adsorbent dose was 0.2 g/L. Then, the suspension was filtered through a 0.45 µm PES syringe filter, and the filtered solution was used to detect the phosphorus concentration. Next, 0.1 mol/L NaOH or HCl were used to adjust the initial pH values of solutions. Since the main form of phosphate in the range of 2.13–7.20 is H₂PO₄⁻ [28], KH₂PO₄ was used as a phosphorus source in the solutions.

All experiments were performed in triplicate. The equilibrium adsorption capacity (q_e , mg/g) and the adsorption capacity at different times t (q_t , mg/g) were calculated as follows:

$$q_e = (C_0 - C_e) V / m \quad (1)$$

$$q_t = (C_0 - C_t) V / m \quad (2)$$

where C_0 (mg/L) represents the initial P concentration, C_e (mg/L) represents the P concentration at equilibrium, and C_t (mg/L) represents the P concentration at time t ; V (L) is the volume of the solution, and m (g) is the adsorbent mass.

To evaluate the equilibrium adsorption parameters, adsorption isotherm experiments were conducted as follows: E-BC dose, 0.2 g/L; initial P concentrations of 10, 20, 50, 70, 100, 150, and 200 mg/L; initial pH, 7.0; adsorption time, 24 h.

Langmuir and Freundlich adsorption isotherm models were used in the study of adsorbent's adsorption isotherms for P in aqueous solutions:

$$\text{Langmuir: } q_e = K_L q_{\max} C_e / (1 + K_L C_e) \quad (3)$$

$$\text{Freundlich: } q_e = K_F C_e^{1/n} \quad (4)$$

In the equations, q_e (mg/g) is the equilibrium adsorption amount, K_L (L/mg) is the Langmuir adsorption equilibrium constant, q_{\max} (mg/g) represents the maximum adsorption capacity, C_e (mg/L) represents P equilibrium concentration, K_F ($\text{mg}^{(1-1/n)} \text{L}^{1/n}/\text{g}$) represents the Freundlich adsorption constant representing the adsorption capacity of the adsorbent, and n represents an indication of linearity. The adsorption isotherms were fitted using the software Origin.8.5 through nonlinear curve fitting.

Adsorption kinetic tests were conducted as follows: E-BC dose, 0.2 g/L; initial P concentration, 100 mg/L; initial pH, 7.0; adsorption time of 5 min, 15 min, 30 min, 60 min, 120 min, 240 min, 360 min, 720 min, and 1440 min.

The pseudo-first-order model and pseudo-second-order model were used in the study of adsorbent's adsorption kinetics for P in aqueous solutions:

$$\text{Pseudo-first-order kinetic equation: } q_t = q_e (1 - e^{-k_1 t}) \quad (5)$$

$$\text{Pseudo-second-order kinetic equation: } t/q_t = 1/k_2 q_e^2 + t/q_e \quad (6)$$

In the equations, q_t is P adsorption amounts at t time, and q_e is P adsorption amounts at equilibrium time; k_1 is the first-order kinetics' adsorption rate constant, and k_2 is the second-order kinetics' adsorption rate constant. The adsorption kinetics were fitted using the software Origin.8.5 through nonlinear curve fitting.

The effects tests of different initial pH on P removal by E-BC were evaluated as follows: E-BC dose, 0.2 g/L; initial P concentration, 100 mg/L; initial pH of 3.0, 5.0, 7.0, 9.0, and 11.0; adsorption time, 24 h.

The effect tests of common competing substances (Cl^- , NO_3^- , SO_4^{2-} , and HCO_3^-) on P removal by E-BC were evaluated as follows: E-BC dose, 0.2 g/L; initial phosphate concentration, 100 mg/L; Cl^- , NO_3^- , SO_4^{2-} and HCO_3^- concentrations, 0.01 mol/L and 0.02 mol/L; adsorption time, 24 h.

Rural residential sewage from a centralized rural sewage treatment facility in Jiaxing (Zhejiang province) was utilized to assess the E-BC adsorbent's suitability for actual phosphorus sewage. Anaerobic-Anoxic-Oxic (A^2O) processes were used in the centralized rural sewage treatment facility; the design capacity was 20 t/d. Every three days, a sample of rural home sewage was taken from the secondary sedimentation tank. Next, 100 mL glass vials that contained 50 mL of rural home sewage and 0.01 g of E-BC material and with stoppers were oscillated (at 180 rpm) in a shaker bath for 4 h at 25 °C.

2.4. Characterization and Analytical Method

The phosphorus concentration of the solution was determined using ammonium molybdate spectral photometry with an ultraviolet spectrophotometer (SHIMADZU UV-2450, Kyoto, Japan) at a wavelength of 700 nm and according to the standard molybdenum blue method [29]. The surface elements and morphologies of adsorbents before and after adsorption of P were studied using scanning electron microscopy with energy dispersive X-ray spectroscopy (SEM-EDS) (Regulus-810, Hitachi, Tokyo, Japan). The diffraction patterns of adsorbents before and after P adsorption were studied by X-ray diffractometer (XRD, Bruker D8 Advance X-ray diffractometer, Karlsruhe, Germany). The XRD patterns were recorded in the 2θ range of 5–90°. The software MDI Jade 6 was used to evaluate the XRD

patterns. A FTIR spectrometer (Thermo Scientific Nicolet IS50, Waltham, MA, USA) was used to study the characterization of the functional groups in the adsorbents before and after P adsorption. The adsorbent samples were mixed with potassium bromide powder and compressed into pellets, and then were characterized over the range from 4000 to 400 cm^{-1} . The fully automated physisorption instrument (JW-BK200B, Beijing, China) was used to detect the specific surface area, pore size, and total pore volume of adsorbents.

3. Results and Discussion

3.1. Sorption of Phosphate on Various E-BC Adsorbents

The effects of the eggshell and pine sawdust's weight ratios as adsorbents on the P adsorbed are presented in Figure 1a. Clearly, the adsorption amounts increased from 72.2 mg/g at eggshell and pine sawdust's weight ratio of 1:2 to 107 mg/g at eggshell and pine sawdust's weight ratio of 2:1. In this study, the lowest P adsorption amount in tested adsorbents was 5.5 mg/g obtained from BC. Clearly, biochar modified by Ca favored P adsorption (Figure 1a); similar results were reported in Luo's research [30]. However, as the weight ratio of eggshell and pine sawdust increased to 3:1, the adsorption amount decreased slightly. Excessive calcium may reduce the adsorption site of the adsorbent. The weight ratio of eggshell and pine sawdust was 2:1 for further experiments.

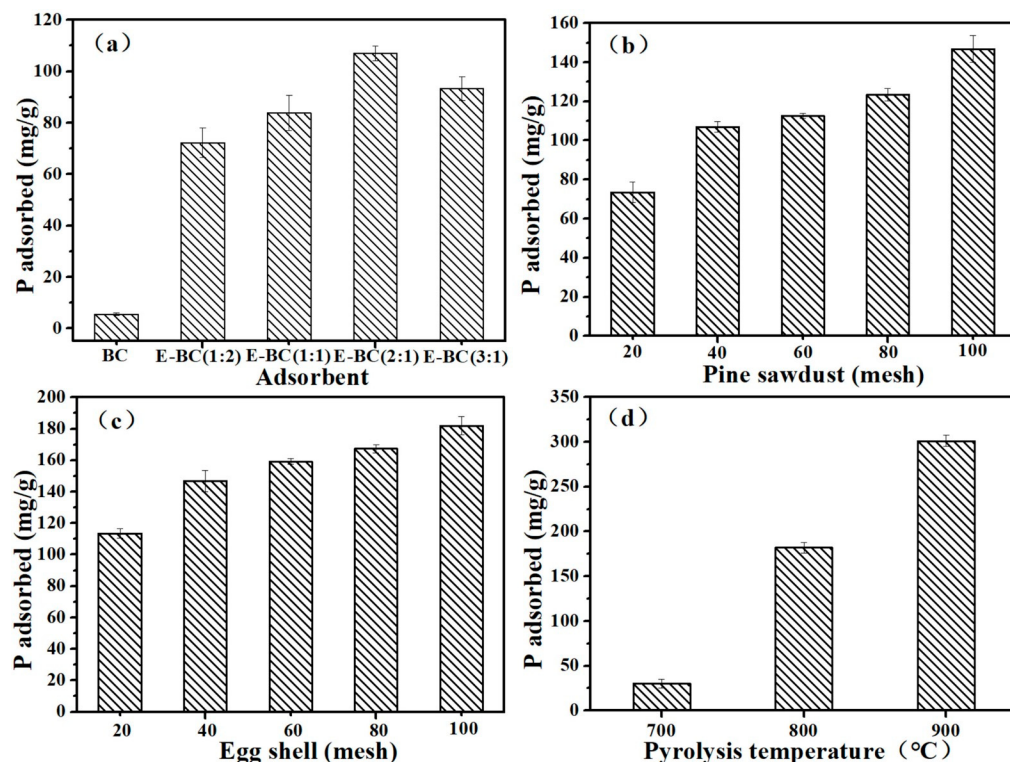


Figure 1. The amount of P adsorbed on various E-BC adsorbents (Dosage: 0.2 g/L; initial P concentration: 100 mg/L; temperature: 25 °C; adsorption time: 24 h; pH = 7), (a) different weight ratio of eggshell and pine sawdust, where eggshell and pine sawdust powder were put through 40 mesh sieves and pyrolysis temperature was 800 °C; (b) pine sawdust powder put through different mesh sieves, the weight ratio of eggshell and pine sawdust was 2:1, eggshell powder put through 40 mesh sieves, and pyrolysis temperature was 800 °C; (c) eggshell powder put through different mesh sieves, the weight ratio of eggshell and pine sawdust was 2:1, pine sawdust powder through 100 mesh sieves, and pyrolysis temperature was 800 °C; (d) different pyrolysis temperatures, the weight ratio of eggshell and pine sawdust was 2:1, and eggshell and pine sawdust powder put through 100 mesh sieves.

Figure 1b presents the effects of pine sawdust powder (through 20–100 mesh sieves) with the fixed eggshell powder that was passed through 40 mesh sieves on the P adsorbed. The adsorption amounts increased from 73.5 mg/g at 20 mesh (0.85 mm) pine sawdust

powder to 146.8 mg/g at 100 mesh (0.15 mm) pine sawdust powder (Figure 1b). Fixed pine sawdust powder for passing through 100 mesh sieves, the effects of eggshell powder (through 20–100 mesh sieves) on the P adsorbed are presented in Figure 1c. The adsorption amounts increased from 113.5 mg/g at 20 mesh (0.85 mm) eggshell powder to 182 mg/g at 100 mesh (0.15 mm) eggshell powder (Figure 1c). It may be that the smaller the particle and the larger the specific surface area of adsorbents, the better the adsorption effect that is obtained.

The adsorption amounts significantly increased, from 30.2 mg/g at a pyrolysis temperature of 700 °C to 301 mg/g at a pyrolysis temperature of 900 °C (Figure 1d). E-BC's adsorption capacity for P increased with an increase in pyrolysis temperature. Since E-BC (2:1)-T900 had the highest adsorption capacity among the preparative E-BC adsorbents, it was selected for further study.

In Table 1, the basic physicochemical properties and major elements of the E-BC samples and BC are shown. It shows that the pore volumes of E-BC (2:1)-T700, E-BC (2:1)-T800, and E-BC (2:1)-T900, increased by 0.019 cm³/g, 0.059 cm³/g, and 0.081 cm³/g, respectively. As the pyrolysis temperature increased, the specific surface area of the E-BC material tended to increase. E-BC (2:1)-T900 had the maximum surface area of 76.565 m²/g among E-BC materials.

Table 1. Specific surface area, pore volume, pore size and major elements of E-BC and BC.

Adsorbent	Physical Properties			Major Elements		
	Specific Surface Area (m ² /g)	Pore Volume (cm ³ /g)	Average Pore Size (nm)	C (%)	O (%)	Ca (%)
E-BC (2:1)-T700	28.960	0.019	2.683	72.16	19.64	5.03
E-BC (2:1)-T800	58.931	0.059	4.031	9.61	59.35	30.95
E-BC (2:1)-T900	76.565	0.081	4.251	7.14	43.9	48.94
BC-T800	18.25	0.021	3.052	79.21	14.85	1.55

The eggshell decomposes into CaO and CO₂ during a high-temperature pyrolysis process [14]. The formation of CO₂ can broaden a material's pore size as an activation substance. In addition, the adsorbent's pore volume and specific surface area may increase when eggshell is added to biochar. The pore volume and surface area of E-BC (2:1)-T800 were higher than those of BC-T800. Biochar's adsorption performance largely depends on its porosity and specific surface area. The larger the adsorbent's specific surface area and the higher the porosity, the more surface adsorption sites there will be and the higher the adsorption performance will be [14,31,32].

With the increase of pyrolysis temperature, the Ca content increased and the C content decreased (Table 1). The mineral structure of eggshells was also altered through pyrolysis [33]. All Ca in eggshell calcined at ≤700 °C existed in the form of calcite (CaCO₃); Ca in eggshells during pyrolysis at 800 °C was composed of lime (CaO), portlandite (Ca(OH)₂), and calcite; Ca in eggshell pyrolysis at 900 °C was composed of lime (CaO) and portlandite (Ca(OH)₂), not calcite [33]. Because CaO and Ca(OH)₂ are more likely to precipitate with P than CaCO₃ [34], P adsorption is considered to increase onto the E-BC (2:1)-T900.

3.2. Adsorption Isotherms

In this study, isotherm experiments were conducted using solutions with different initial P concentrations (10, 20, 50, 70, 100, 150, and 200 mg/L). Langmuir and Freundlich adsorption isotherm models were used in the study of E-BC (2:1)-T900's adsorption isotherms for P in aqueous solutions.

The fitted adsorption isotherms of P onto the E-BC (2:1)-T900 materials are shown in Figure 2. The fitting effect of the Langmuir model on experimental data is better than that of the Freundlich model in this study (Figure 2). The corresponding fitting parameters for Langmuir model were q_{max} = 302.9 mg/g, K_L = 4.1 L/mg, R² = 0.999. The corre-

sponding fitting parameters for the Freundlich model were $K_F = 115.1 \text{ mg}^{(1 - 1/n)L^{1/n}}/\text{g}$, $1/n = 0.33 \text{ L/mg}$, $R^2 = 0.947$. Furthermore, the regression coefficients (R^2) for the Langmuir model were higher than the Freundlich model, further confirming that the Langmuir isotherm model adequately described the experimental data regarding the adsorption of P onto E-BC, implying that the effective adsorption surface of E-BC (2:1)-T900 in the process of adsorbing P was monolayer and homogeneous, similar to the P adsorption behavior reported for other research on Ca-based adsorbents [14,16].

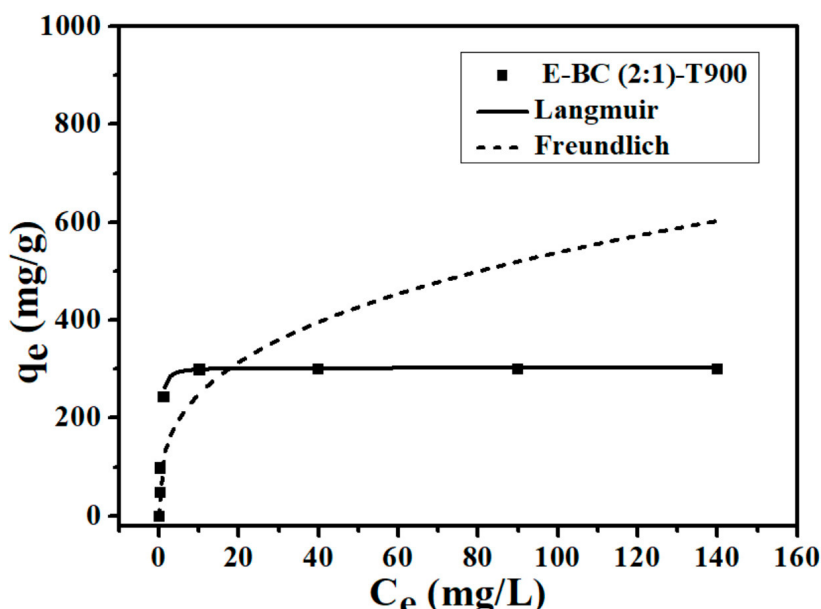


Figure 2. P adsorption isotherms onto E-BC (2:1)-T900 (Dosage: 0.2 g/L; temperature: 25 °C; adsorption time: 24 h; pH = 7).

The q_{\max} of E-BC (2:1)-T900 calculated by the Langmuir isotherm was 302.9 mg/g, which was consistent with the experimental maximum adsorption capacity of 301 mg/g. Recently, the modified biochar synthesized from cheap, calcium-rich waste has achieved a good P adsorption effect. For example, tobacco straw was employed as a carbon source and oyster shell was used as a Ca source to create a modified-biochar adsorbent with a maximum P adsorption capacity of 88.64 mg/g [14]. In another study, marble waste was employed as a Ca source and agricultural waste was used as a carbon source to synthesize modified-biochar composites for removing P from waste streams; the maximum P removal capacity of these composites was 263.17 mg/g [17]. When rice straw was employed as the carbon source and eggshell was used as the source of Ca, a modified-biochar adsorbent with a maximum P adsorption capacity of 231 mg/g was created [35]. In this study, the prepared E-BC (2:1)-T900 adsorbent material's maximum adsorption capacity of P (301 mg/g) was higher than the adsorbents reported in the above studies, indicated that the E-BC adsorbents in aqueous solution had excellent adsorption properties for removing P.

3.3. Adsorption Kinetics

Figure 3 illustrates the results of the kinetic behavior of phosphate on E-BC (2:1)-T900. Clearly, during the initial 1 h, the adsorption processes of E-BC (2:1)-T900 for P were rapid, and then slowed down until they reached equilibrium, within 4 h. The adsorption process involves an initial rapid diffusion of ions from the solution to the external adsorbent surfaces, followed by a slower adsorption process by diffusion of ions into the pores of the inner adsorbent surfaces [35].

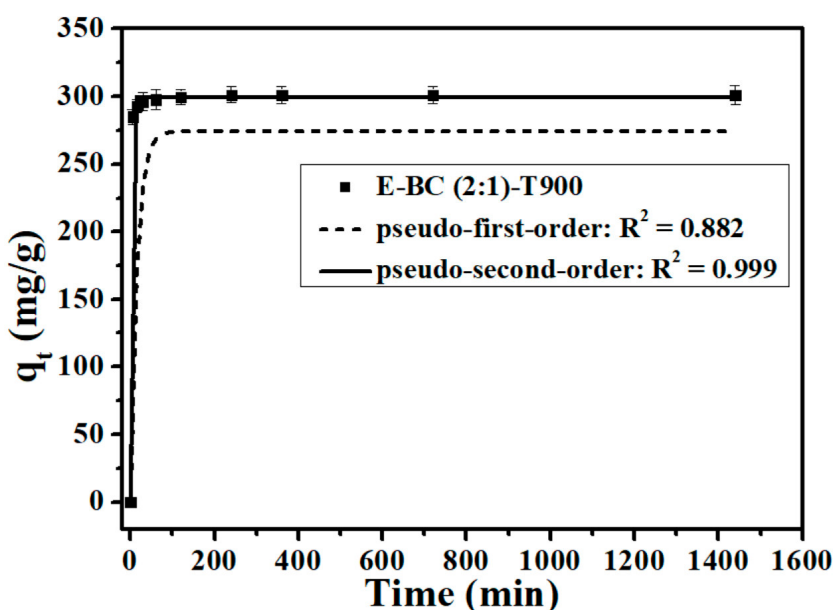


Figure 3. P adsorption kinetics onto E-BC (2:1)-T900 (Dosage: 0.2 g/L; temperature: 25 °C; initial P concentration: 100 mg/L; pH = 7).

The pseudo-first-order model and pseudo-second-order model were used in the study of E-BC (2:1)-T900's adsorption kinetics for P. The results showed that the coefficient of determination simulated with the pseudo-second order model ($R^2 = 0.999$) is higher than the pseudo-first-order model ($R^2 = 0.882$) (Figure 3), which suggested that the pseudo-second-order kinetic model can accurately describe the adsorption kinetic process of P onto E-BC (2:1)-T900, and a monolayer chemisorption occurred on the adsorbent surface, which was consistent with the above isotherm result depicted by the Langmuir model. Based on the analysis of the pseudo-second-order theory and the chemisorption characteristics of E-BC (2:1)-T900, chemisorption was the main rate-limiting step of P adsorption by E-BC (2:1)-T900. Compared to the pseudo-first-order model, the pseudo-second-order kinetic model can accurately describe the adsorption kinetic process of P onto Ca-modified biochar that has been reported in other studies, indicating that chemisorption is the dominant process during P adsorption on Ca-modified biochar [14,17,35,36], which involves the sharing of electrons between Ca-modified biochar and P to form a new compound or covalent bond [17,35]; in addition to chemical adsorption, electrostatic attraction and interactions can also occur.

3.4. Effect of pH

The pH of the environment is an important factor in the adsorption process. The effect of solution pH on the adsorption of P onto E-BC (2:1)-T900 was examined. The P adsorption amount on E-BC (2:1)-T900 increased from 292.2 mg/g at pH = 3 to 301 mg/g at pH = 7 (Figure 4), and the P adsorption amount on E-BC (2:1)-T900 slightly decreased to 298.5 mg/g at pH = 9 and 296.7 mg/g at pH = 11 (Figure 4). Thus, over a wide initial pH range of 3–11, the E-BC (2:1)-T900 showed a good adsorption effect on P.

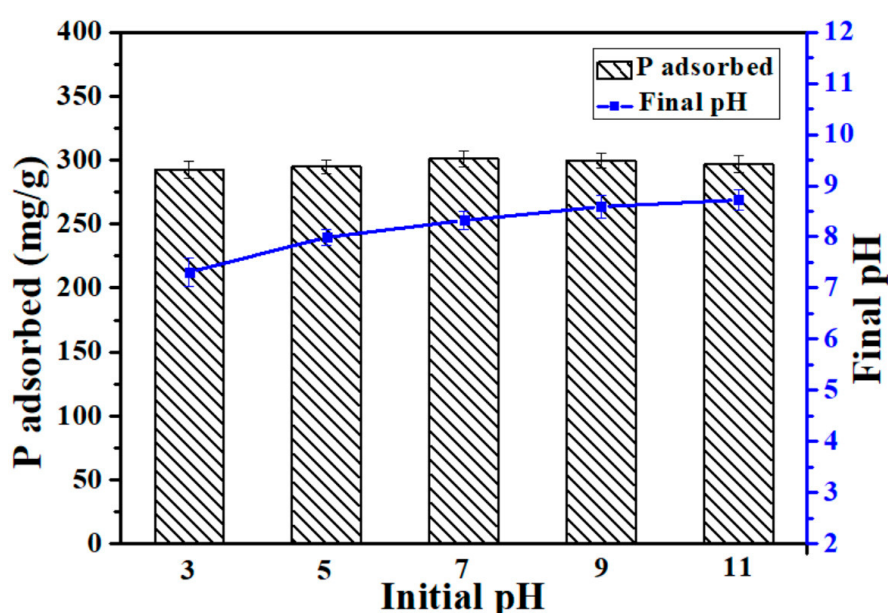


Figure 4. The effect of initial pH on P adsorption capacity of E-BC (2:1)-T900 (Dosage: 0.2 g/L; temperature: 25 °C; adsorption time: 24 h; initial P concentration: 100 mg/L).

The ionization balance of P can be influenced by solution pH; at different pH values, the phosphate forms are different, so the adsorption effect of the adsorbent for P may be affected. The phosphate species present in aqueous solutions are H_3PO_4 ($\text{pH} < 2.15$), H_2PO_4^- ($2.15 < \text{pH} < 7.20$), HPO_4^{2-} ($7.20 < \text{pH} < 12.33$), and PO_4^{3-} ($\text{pH} > 12.33$), depending on the pH [28]. Above the three phosphate forms, the PO_4^{3-} is most easily adsorbed onto the surface of the adsorbent, followed by the HPO_4^{2-} . This is due to the presence of H^+ , which can hinder the complexion of P with Ca [16,17], indicating that the presence of H^+ most likely occupies active binding sites for P [16,35]. In addition, calcium active components contribute to the adsorption of P onto the E-BC (2:1)-T900 through strong chemical interaction mechanisms, resulting in the high adsorption capacity of the E-BC (2:1)-T900 for P over a wide pH range (3–11). As for the effect of pH on the phosphorus adsorption by E-BC (2:1)-T900 adsorbent material, an in-depth mechanism study should be carried out in our future experiments. Similarly, in the Deng et al. study, over a wide initial pH range of 3–11, Ca-biochar synthesis from marble waste showed a good adsorption effect on P [17]. Over a wide initial pH range of 1–11, the black-liquor-derived Ca-activated biochar showed a good adsorption effect on P in the Liu et al. report [37].

3.5. Influence of coexisting anions

In natural water and wastewater, some common anions may compete for adsorption sites with P [38]. In this study, the concentrations of different coexisting anions Cl^- , NO_3^- , SO_4^{2-} , and HCO_3^- (10, 20) mM were much higher than the initial P concentration of 100 mg/L (3.23 mM) (Figure 5). The common anions have different levels of effect on the P adsorption capacity of the E-BC (2:1)-T900, following the order $\text{HCO}_3^- > \text{SO}_4^{2-} > \text{NO}_3^- > \text{Cl}^-$. The results showed that the anions Cl^- , NO_3^- , and SO_4^{2-} had a limited effect on the adsorption process of P; even at high ion concentrations of up to 20 mmol/L for Cl^- and NO_3^- , the adsorption capacity of P remained at 297.3 mg/g and 296.2 mg/g, respectively. As the concentration of SO_4^{2-} was gradually increased from blank control to 10 mM and 20 mM, the adsorption capacity of E-BC (2:1)-T900 decreased from 301 to 295.2 and 283.5 mg/g, respectively, and the removal rate of P slightly decreased from 60.2% at blank control to 59% and 56.7%, respectively.

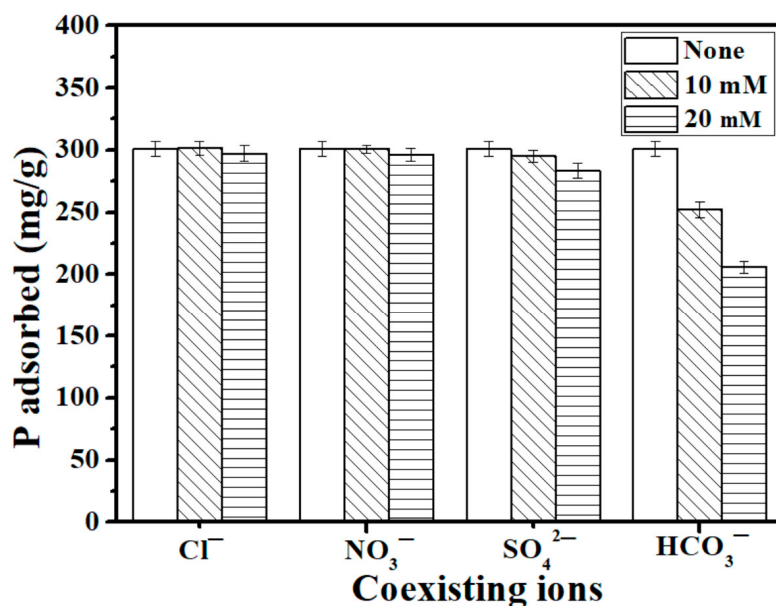


Figure 5. Effect of co-existing ions (Cl^- , NO_3^- , SO_4^{2-} , and HCO_3^-) on P adsorption capacity of E-BC (2:1)-T900 (Dosage: 0.2 g/L; temperature: 25 °C; adsorption time: 24 h; initial P concentration: 100 mg/L).

On the other hand, HCO_3^- had a significant negative effect on the adsorption of P onto the E-BC (2:1)-T900 adsorbent. When the concentration of HCO_3^- was gradually increasing, the P adsorption amount of the E-BC (2:1)-T900 adsorbent had a significant downward trend. The HCO_3^- ionization in the solution can generate CO_3^{2-} , and the adsorption sites in E-BC (2:1)-T900 are reduced because CO_3^{2-} competes with P to bind Ca and produce precipitation. Similar results have been reported in the study of other calcium-rich phosphate adsorbents [35,37]. However, when the concentration of HCO_3^- was as high as 20 mM, the phosphate adsorption amount of E-BC (2:1)-T900 still reached 205.8 mg/g. Thus, the E-BC (2:1)-T900 has higher adsorption selectivity for phosphate anions than for many other common anions. The above results show that E-BC (2:1)-T900 has significant potential in practical P-containing wastewater applications, even in the presence of Cl^- , NO_3^- , SO_4^{2-} , and HCO_3^- common ions. Similar, in the Liu et al. study, the common anions also have different levels of effect on the P adsorption capacity of the CaO-biochar adsorbent, following the order $\text{HCO}_3^- > \text{SO}_4^{2-} > \text{NO}_3^- > \text{Cl}^-$ [35]. As for the effect of coexisting anions on the P adsorption by E-BC (2:1)-T900, study of the in-depth mechanism should be carried out in future experiments.

3.6. Adsorption Mechanisms

The adsorbents before and after the adsorption of P were analyzed by XRD, SEM, and FTIR to explore the adsorption mechanism of P on E-BC (2:1)-T900. The characteristic peaks of E-BC (2:1)-T900 before and after adsorption P showed a significant change by the FTIR spectra analysis (Figure 6). The peaks at 875 cm^{-1} (C-O) and 1410 cm^{-1} (C=C) were observed for the adsorbent before and after adsorption [14], suggested that the C-O and C=C group did not contribute to the adsorption of P. Before adsorption, the peak at 3641 cm^{-1} (O-H) was attributed to Ca(OH)_2 for E-BC (2:1)-T900 [36]. After adsorption, the peak at 3641 cm^{-1} vanished, and it was shown that the -OH took part in the chemical adsorption process of P. Furthermore, the emerged peaks at 560 , 600 , 963 , and 1022 cm^{-1} (P-O) were considered to be phosphates [14], which showed that P was adsorbed onto E-BC (2:1)-T900. Similar results were reported by other researchers [14,17,35].

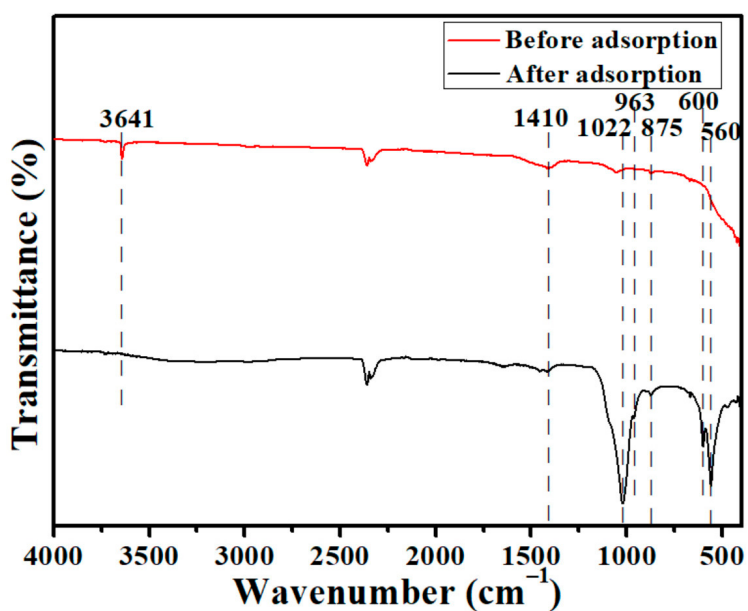


Figure 6. The FTIR spectra of E-BC (2:1)-T900 before and after P adsorption.

The diffraction patterns of E-BC (2:1)-T900 before and after adsorption of P showed a significant change by XRD spectra analysis (Figure 7). Before adsorption, E-BC (2:1)-T900 had CaO's characteristic peaks (PDF #37-1497, $2\theta = 32.2^\circ, 37.5^\circ, 54.0^\circ, 64.4^\circ, 67.6^\circ, 79.9^\circ, 88.7^\circ$) and Ca(OH)₂'s characteristic peaks (PDF #04-0733, $2\theta = 18.1^\circ, 28.7^\circ, 34.2^\circ, 47.1^\circ, 50.9^\circ$). CaO and Ca(OH)₂ are active sites in the E-BC (2:1)-T900 for P adsorption. The above results showed that Ca from the eggshell was successfully introduced into E-BC (2:1)-T900 materials and exists in the forms of CaO and Ca(OH)₂. CaO was produced by the calcination of CaCO₃ in the eggshell. Ca(OH)₂ was produced from a part of CaO hydrates with H₂O in the environment. After adsorption, the diffraction peaks of CaO and Ca(OH)₂ vanished, and E-BC (2:1)-T900 had Ca₅(PO₄)₃OH's characteristic peaks (PDF #09-0432, $2\theta = 25.9^\circ, 29^\circ, 32.2^\circ, 39.8^\circ, 46.7^\circ, 49.5^\circ, 53.2^\circ, 64.2^\circ$). The Ca₅(PO₄)₃OH is generated from the reaction of phosphate with CaO or Ca(OH)₂.

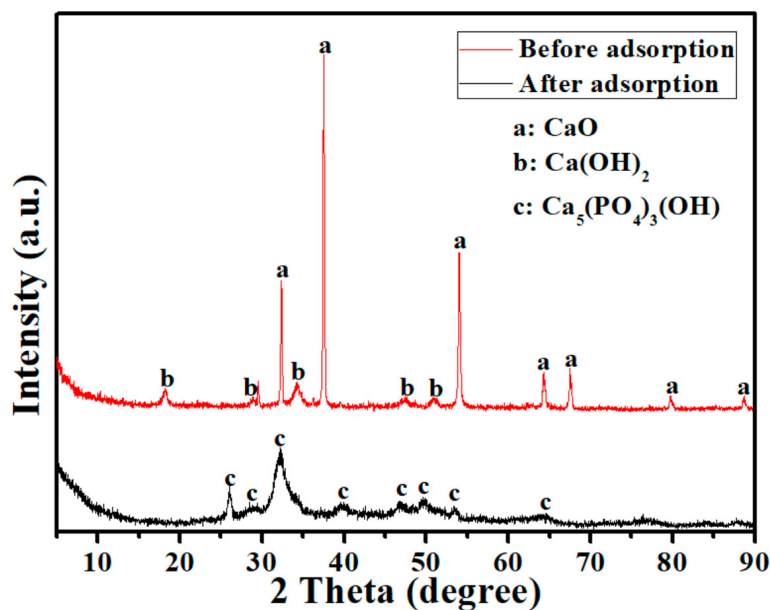


Figure 7. X-ray diffraction pattern of E-BC (2:1)-T900 before and after P adsorption.

The morphologies of E-BC (2:1)-T900 before and after adsorption P showed a significant change through SEM images (Figure 8). Before the adsorption of P, the surface of E-BC (2:1)-T900 was relatively clean, while many impurity particles appeared on the surface of E-BC (2:1)-T900, such as CaO and Ca(OH)₂. In addition, E-BC (2:1)-T900 had a porous structure before adsorption. After the adsorption of P, many flocculent materials appeared on the surface of the adsorbents; the pores of E-BC (2:1)-T900 were blocked, indicated that CaO or Ca(OH)₂ on the E-BC (2:1)-T900 introduced by the eggshells could have a chemical reaction with P. As seen in Figure 8c, after adsorption of P, the phosphorus element is distributed on the E-BC (2:1)-T900 (major elements: P 14.39%; Ca 25.83%; O 43.47%). Therefore, combined with Figure 7, it can be inferred that the newly formed compound on the E-BC (2:1)-T900 should be Ca₅(PO₄)₃OH.

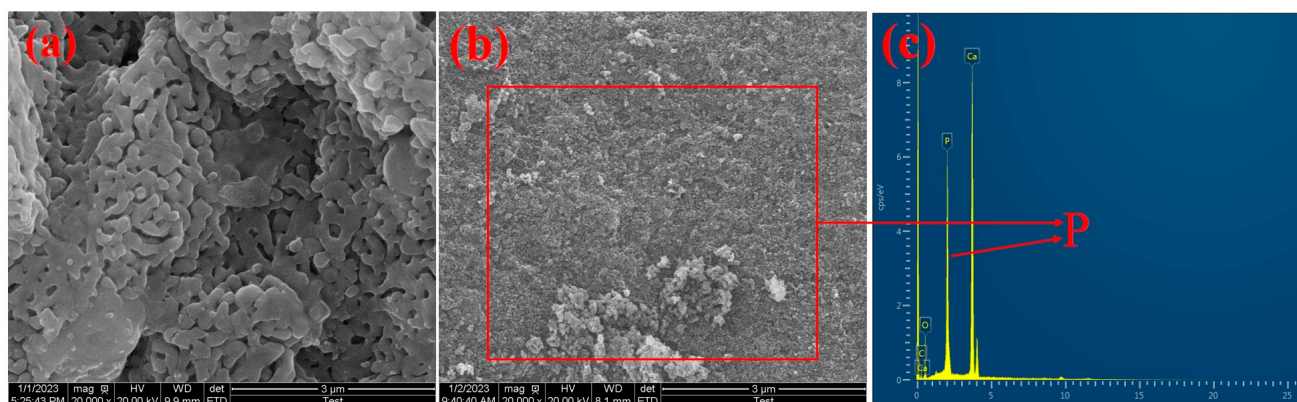


Figure 8. SEM photographs of E-BC (2:1)-T900 (a) before P adsorption; (b) after P adsorption; (c) EDS image of E-BC (2:1)-T900 after P adsorption.

According to the above results, the mechanisms by which E-BC (2:1)-T900 adsorbs P include physical adsorption and chemisorption. The dominant sorption mechanism of E-BC (2:1)-T900 for P was chemisorption; CaO or Ca(OH)₂ reacted with phosphate to form Ca₅(PO₄)₃OH, and the result was similar to other studies [17,35].

3.7. Removal of Phosphate by E-BC (2:1)-T900 from Rural Domestic Sewage

Figure 9 shows that the discharge of total phosphorus (TP) in rural domestic sewage of the centralized rural sewage treatment facility (design capacity 20 t/d) in all but one sampling batches exceeded the second-grade Discharge Standard (DB33/973-2021) [39] (TP < 3 mg/L) in this study. Figure 9 presents the results of phosphate adsorption by adding 0.01 g E-BC (2:1)-T900 to 50 mL of actual rural sewage. The TP content in the rural domestic sewage was 2.41–11.5 mg/L; after adsorption, the TP content was 0.019–0.33 mg/L, and the TP removal rate reached 95.3–99.5%. After adsorption treatment, the discharge of TP in rural sewage in all sampling batches met the second-grade Discharge Standard (DB33/973-2021) (TP < 3 mg/L), and even met the first-grade Discharge Standard of Water Pollutants for Centralized Rural Sewage Treatment Facilities (DB33/973-2021) [39] (TP < 2 mg/L).

Many complex components may be present in the actual wastewater, which can interfere with P removal by the adsorbent. In this study, the E-BC (2:1)-T900 materials also exhibited high P adsorption capacity under actual rural sewage. Therefore, the E-BC (2:1)-T900 adsorbent should have great potential in the treatment of large-scale P-containing rural sewage.

The main components of E-BC (2:1)-T900 biochar materials are O, C, Ca, and H. These elements are environmentally friendly, and the adsorbents have a mesoporous structure. After adsorption of P, a good deal of Ca₅(PO₄)₃(OH) is produced on the E-BC (2:1)-T900, which is rich in P, and also has the physical properties of biochar. Therefore, the P-adsorbed E-BC (2:1)-T900 sample may be further used as a soil regulator and fertilizer. This method

can realize the reuse of E-BC (2:1)-T900 and the virtuous cycle of phosphorus resources in the ecosystem [17,35,37].

The cost of raw material for adsorbents is one of the important factors influencing their practical application. In this study, the E-BC adsorbent was prepared from waste materials, so the cost of raw material is low. However, apart from the cost of raw materials, the energy cost of calcination is another of the major costs in the preparation of biochar adsorbents. Therefore, the removal effect of P, the cost of using E-C adsorbent, and the benefit of P recovery should be comprehensively evaluated in the future possible engineering application of rural domestic sewage treatment.

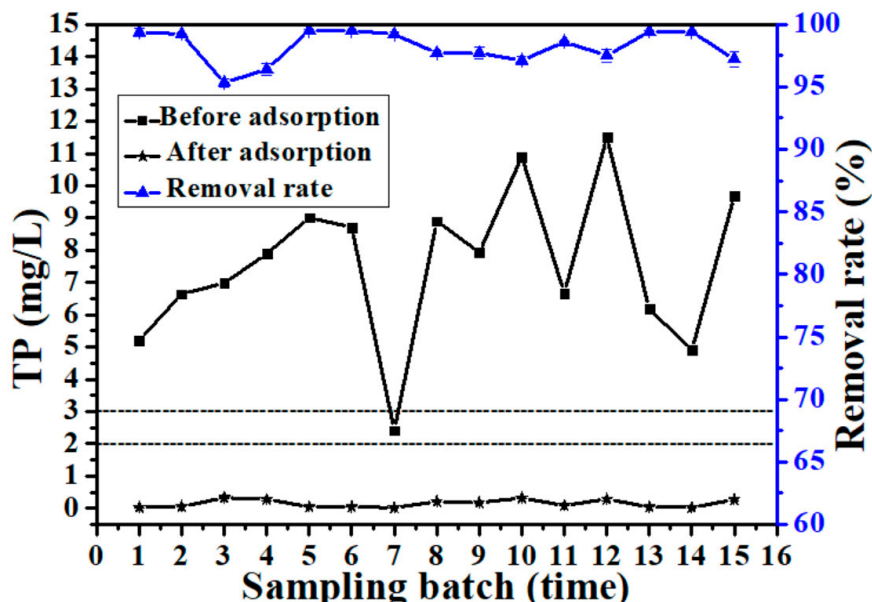


Figure 9. The removal rate of TP in rural domestic sewage by E-BC (2:1)-T900 (Dosage: 0.2 g/L; temperature: 25 °C; adsorption time: 4 h).

4. Conclusions

In this study, in order to improve TP treatment efficiency for meeting discharge standards in rural regions, Ca-modified biochar (E-BC) adsorbents were prepared by a one-step pyrolysis method that utilized eggshell waste and waste pine sawdust as raw materials. The mass ratio of eggshell and sawdust, eggshell and sawdust powder passing through different mesh sieves, and the optimum pyrolysis temperature were determined.

The E-BC adsorbents were used to remove P from aqueous solutions, and the results showed that the prepared E-BC composites exhibited excellent adsorption capacity and adsorption selectivity. The maximum adsorption capacity of 301 mg/g was obtained by the E-BC sample that was prepared from eggshell (100 mesh) and pine sawdust (100 mesh) with a mass ratio of 2:1 and a pyrolysis temperature of 900 °C. CaO and Ca(OH)₂ react with phosphate to generate Ca₅(PO₄)₃OH, which plays a prominent role in adsorbing phosphate. E-BC can effectively remove P from rural domestic sewage. The removal rate of TP in rural domestic sewage ranges from 95.3 to 99.5%. After adsorption treatment, the discharge of TP in rural sewage meets the second-grade Discharge Standard (DB33/973-2021) (TP < 3 mg/L), and even the first-grade Discharge Standard (DB33/973-2021) (TP < 2 mg/L).

Author Contributions: C.X. conducted the analysis of the data as well as the data modeling and wrote the paper; R.L., L.C. and Q.W. contributed to the writing of the paper; C.X., Y.H. and Q.T. obtained the experimental data. All authors have read and agreed to the published version of the manuscript.

Funding: This research was supported by the National Key Research and Development Program of China (No.2020YFD1100103-2), Leading Talent of the Science & Technology Nova Program of Zhejiang (2020R52039), and Outstanding Innovative Team Supporting Plan of Jiaxing City.

Data Availability Statement: Not applicable.

Conflicts of Interest: The authors declare no conflict of interest.

References

1. Gonzalez-Tineo, P.A.; Durán-Hinojosa, U.; Delgadillo-Mirquez, L.R.; Meza-Escalante, E.R.; Gortáres-Moroyoqui, P.; Ulloa-Mercado, R.G.; Serrano-Palacios, D. Performance improvement of an integrated anaerobic-aerobic hybrid reactor for the treatment of swine wastewater. *J. Water Process Eng.* **2020**, *34*, 101164. [\[CrossRef\]](#)
2. Yang, F.L.; Zhang, H.R.; Zhang, X.Z.; Zhang, Y.; Li, J.H.; Jin, F.M.; Zhou, B.X. Performance analysis and evaluation of the 146 rural decentralized wastewater treatment facilities surrounding the Erhai Lake. *J. Clean. Prod.* **2021**, *315*, 128159. [\[CrossRef\]](#)
3. Zong, Y.T.; Chen, H.; Malik, Z.; Xiao, Q.; Lu, S.G. Comparative study on the potential risk of contaminated-rice straw, its derived biochar and phosphorus modified biochar as an amendment and their implication for environment. *Environ. Pollut.* **2022**, *293*, 118515. [\[CrossRef\]](#)
4. Chen, Z.H.; Wu, Y.H.; Huang, Y.P.; Song, L.X.; Chen, H.F.; Zhu, S.J.; Tang, C.L. Enhanced adsorption of phosphate on orange peel-based biochar activated by Ca/Zn composite: Adsorption efficiency and mechanisms. *Collids Surf. A* **2022**, *651*, 129728. [\[CrossRef\]](#)
5. Zhang, M.D.; He, M.Z.; Chen, Q.P.; Huang, Y.L.; Zhang, C.Y.; Yue, C.; Yang, L.Y.; Mu, J.L. Feasible synthesis of a novel and low-cost seawater-modified biochar and its potential application in phosphate removal/recovery from wastewater. *Sci. Total Environ.* **2022**, *824*, 153833. [\[CrossRef\]](#) [\[PubMed\]](#)
6. Cao, H.; Wu, X.; Syed-Hassan, S.S.; Zhang, S.; Mood, S.H.; Milan, Y.J.; Garcia-Perez, M. Characteristics and mechanisms of phosphorous adsorption by rape straw-derived biochar functionalized with calcium from eggshell. *Bioresour. Technol.* **2020**, *318*, 124063. [\[CrossRef\]](#)
7. Caneghem, J.V.; Brems, A.; Lievens, P.; Block, C.; Billen, P.; Vermeulen, I.; Dewil, R.; Baeyens, J.; Vandecasteele, C. Potential of pistachio shell biochar and dicalcium phosphate combination to reduce Pb speciation in spinach, improved soil enzymatic activities, plant nutritional quality, and antioxidant defense system. *Chemosphere* **2020**, *245*, 125611.
8. Yang, J.; Zhang, M.L.; Wang, H.X.; Xue, J.B.; Lv, Q.; Pang, G.B. Efficient Recovery of Phosphate from Aqueous Solution Using Biochar Derived from Co-pyrolysis of Sewage Sludge with Eggshell. *J. Environ. Chem. Eng.* **2021**, *9*, 105354. [\[CrossRef\]](#)
9. Agegnehu, G.; Bass, A.M.; Nelson, P.N.; Bird, M.I. Benefits of biochar, compost and biochar-compost for soil quality, maize yield and greenhouse gas emissions in a tropical agricultural soil. *Sci. Total Environ.* **2016**, *543*, 295–306. [\[CrossRef\]](#)
10. Novais, S.V.; Zenero, M.D.O.; Conz, R.F.; Cerri, C.E.P.; Tronto, J. Poultry manure and sugarcane straw biochars modified with MgCl₂ for phosphorus adsorption. *J. Environ. Manag.* **2018**, *214*, 36–44. [\[CrossRef\]](#)
11. Cheng, F.L.; Wang, Y.N.; Fan, Y.T.; Huang, D.; Pan, J.; Li, W. Optimized Ca-Al-La modified biochar with rapid and efficient phosphate removal performance and excellent pH stability. *Arab. J. Chem.* **2023**, *16*, 104880. [\[CrossRef\]](#)
12. Feng, Y.Y.; Luo, Y.N.; He, Q.P.; Zhao, D.; Zhang, K.Q.; Shen, S.Z.; Wang, F. Performance and mechanism of a biochar-based Ca-La composite for the adsorption of phosphate from water. *J. Environ. Chem. Eng.* **2021**, *9*, 105267. [\[CrossRef\]](#)
13. Wang, C.W.; Qiu, C.; Song, Z.G.; Gao, M.L. A novel Ca/Mn-modified biochar recycles P from solution: Mechanisms and phosphate efficiency. *Environ. Sci. Process. Impacts* **2022**, *24*, 474–485. [\[CrossRef\]](#) [\[PubMed\]](#)
14. Feng, M.H.; Li, M.M.; Zhang, L.S.; Luo, Y.; Zhao, D.; Yuan, M.Y.; Zhang, K.Q.; Wang, F. Oyster Shell Modified Tobacco Straw Biochar: Efficient Phosphate Adsorption at Wide Range of pH Values. *Int. J. Environ. Res. Public Health* **2022**, *19*, 7227. [\[CrossRef\]](#)
15. Missau, J.S.; Rodriguesb, M.A.; Bertuola, D.A.; Tanabea, E.H. Phosphate adsorption improvement using a novel adsorbent by CaFe/LDH supported onto CO₂ activated biochar. *Water Sci. Technol.* **2022**, *86*, 2396–2414. [\[CrossRef\]](#) [\[PubMed\]](#)
16. Wang, S.D.; Kong, L.J.; Long, J.Y.; Su, M.H.; Diao, Z.H.; Chang, X.Y.; Chen, D.Y.; Song, G.; Shih, K. Adsorption of phosphorus by calcium-flour biochar: Isotherm, kinetic and transformation studies. *Chemosphere* **2018**, *195*, 666–672. [\[CrossRef\]](#)
17. Deng, W.D.; Zhang, D.Q.; Zheng, X.X.; Ye, X.Y.; Niu, X.J.; Lin, Z.; Fu, M.L.; Zhou, S.Q. Adsorption recovery of phosphate from waste streams by Ca/Mg biochar synthesis from marble waste, calcium-rich sepiolite and bagasse. *J. Clean. Prod.* **2021**, *288*, 125638. [\[CrossRef\]](#)
18. Liu, D.D.; Hao, Z.K.; Chen, D.Q.; Jiang, L.P.; Li, T.Q.; Tian, B.; Yan, C.Q.; Luo, Y.; Chen, G.; Ai, H.F. Use of eggshell-catalyzed biochar adsorbents for Pb removal from aqueous solution. *ACS Omega* **2022**, *7*, 21808–21819. [\[CrossRef\]](#)
19. Waheed, M.; Yousaf, M.; Shehzad, A.; Inam-Ur-Raheem, M.; Kashif Iqbal Khan, M.; Rafiq Khan, M.; Ahmad, N.; Abdullah; Muhammad Aadil, R. Channelling eggshell waste to valuable and utilizable products: A comprehensive review. *Trends Food Sci. Technol.* **2020**, *106*, 78–90. [\[CrossRef\]](#)
20. Luo, J.Y.; Huang, W.X.; Guo, W.; Ge, R.; Zhang, Q.; Fang, F.; Feng, Q.; Cao, J.S.; Wu, Y. Novel strategy to stimulate the food wastes anaerobic fermentation performance by eggshell wastes conditioning and the underlying mechanisms. *Chem. Eng. J.* **2020**, *398*, 125560. [\[CrossRef\]](#)
21. Matej, B.; Elena, V.B.; Dmitry, R.; Stefan, P.; Daily, R.P.; Tihana, M.; Rafael, L. State-of-the-art of eggshell waste in materials science: Recent advances in catalysis, pharmaceutical applications, and mechanochemistry. *Trends Food Sci. Technol.* **2021**, *8*, 612567.

22. Li, C.; Zhou, S.X.; Li, Q.Y.; Gao, G.M.; Zhang, L.J.; Zhang, S.; Huang, Y.; Ding, K.; Hu, X. Activation of sawdust with eggshells. *J. Anal. Appl. Pyrol.* **2023**, *171*, 105968. [[CrossRef](#)]
23. Zhang, Z.; Shen, Q.; Cissoko, N.; Wo, J.; Xu, X. Removal of phosphates using eggshells and calcined eggshells in high phosphate solutions. *Appl. Biol. Chem.* **2022**, *65*, 75. [[CrossRef](#)]
24. Sarker, P.; Liu, X.; Hata, N.; Takeshita, H.; Miyamura, H.; Maruo, M. Thermally modified bamboo-eggshell adsorbent for phosphate recovery and its sustainable application as fertilizer. *Environ. Res.* **2023**, *231*, 115992. [[CrossRef](#)] [[PubMed](#)]
25. Liu, J.; Korpinen, R.; Mikkonen, K.S.; Willför, S.; Xu, C.L. Nanofibrillated cellulose originated from birch sawdust after sequential extractions: A promising polymeric material from waste to films. *Cellulose* **2014**, *21*, 2587–2598. [[CrossRef](#)]
26. Shaheen, T.I.; Emam, H.E. Sono-chemical synthesis of cellulose nanocrystals from wood sawdust using acid hydrolysis. *Int. J. Biol. Macromol.* **2018**, *107*, 1599–1606. [[CrossRef](#)]
27. Dong, X.F.; Gan, W.T.; Shang, Y.; Tang, J.F.; Wang, Y.X.; Cao, Z.F.; Xie, Y.J.; Liu, J.Q.; Bai, L.; Li, J.; et al. Low-value wood for sustainable high-performance structural materials. *Nat. Sustain.* **2022**, *5*, 628–635. [[CrossRef](#)]
28. Xie, F.Z.; Wu, F.C.; Liu, G.J.; Mu, Y.S.; Feng, C.L.; Wang, H.H.; Giesy, J.P. Removal of phosphate from eutrophic lakes through adsorption by in situ formation of magnesium hydroxide from diatomite. *Environ. Sci. Technol.* **2014**, *48*, 582–590. [[CrossRef](#)]
29. Pan, W.L.; Xie, H.M.; Zhou, Y.; Wu, Q.Y.; Zhou, J.Q.; Guo, X. Simultaneous adsorption removal of organic and inorganic phosphorus from discharged circulating cooling water on biochar derived from agricultural waste. *J. Clean. Prod.* **2023**, *383*, 135496. [[CrossRef](#)]
30. Luo, D.; Wang, L.Y.; Nan, H.Y.; Cao, Y.J.; Wang, H.; Kumar, T.V.; Wang, C.Q. Phosphorus adsorption by functionalized biochar: A review. *Environ. Chem. Lett.* **2023**, *21*, 497–524. [[CrossRef](#)]
31. Bacelo, H.; Pintor, A.M.; Santos, S.C.; Boaventura, R.A.; Botelho, C.M. Performance and prospects of different adsorbents for phosphorus uptake and recovery from water. *Chem. Eng. J.* **2020**, *381*, 122566. [[CrossRef](#)]
32. Liu, M.C.; Wang, C.Z.; Guo, J.B.; Zhang, L.H. Removal of phosphate from wastewater by lanthanum modified bio-ceramisite. *J. Environ. Chem. Eng.* **2021**, *9*, 106123. [[CrossRef](#)]
33. Lee, J.I.; Kim, J.M.; Yoo, S.C.; Jho, E.H.; Lee, C.G.; Park, S.J. Restoring phosphorus from water to soil: Using calcined eggshells for P adsorption and subsequent application of the adsorbent as a P fertilizer. *Chemosphere* **2022**, *287*, 132267. [[CrossRef](#)]
34. Khemthong, P.; Luadthong, C.; Nualpaeng, W. Industrial eggshell wastes as the heterogeneous catalysts for microwave-assisted biodiesel production. *Catal. Today* **2012**, *190*, 112–116. [[CrossRef](#)]
35. Liu, X.N.; Shen, F.; Qi, X.H. Adsorption recovery of phosphate from aqueous solution by CaO-biochar composites prepared from eggshell and rice straw. *Sci. Total Environ.* **2019**, *666*, 694–702. [[CrossRef](#)]
36. Mitrogiannis, D.; Psychoyou, M.; Baziotis, I.; Inglezakis, V.J.; Koukouzas, N.; Tsoukalas, N.; Palles, D.; Kamitsos, E.; Oikonomou, G.; Markou, G. Removal of phosphate from aqueous solutions by adsorption onto $\text{Ca}(\text{OH})_2$ treated natural clinoptilolite. *Chem. Eng. J.* **2017**, *320*, 510–522. [[CrossRef](#)]
37. Liu, X.N.; Shen, F.; Smith, R.L., Jr.; Qi, X.H. Black liquor-derived calcium-activated biochar for recovery of phosphate from aqueous solutions. *Bioresour. Technol.* **2019**, *294*, 122198. [[CrossRef](#)] [[PubMed](#)]
38. Zhuo, S.N.; Dai, T.C.; Ren, H.Y.; Liu, B.F. Simultaneous adsorption of phosphate and tetracycline by calcium modified corn stover biochar: Performance and mechanism. *Bioresour. Technol.* **2022**, *359*, 127477. [[CrossRef](#)]
39. DB33/973-2021; Discharge Standard of Water Pollutants for Centralized Rural Sewage Treatment Facilities. The People's Government of Zhejiang Province: Hangzhou, China, 2021. (In Chinese)

Disclaimer/Publisher's Note: The statements, opinions and data contained in all publications are solely those of the individual author(s) and contributor(s) and not of MDPI and/or the editor(s). MDPI and/or the editor(s) disclaim responsibility for any injury to people or property resulting from any ideas, methods, instructions or products referred to in the content.